Synthesis and Self-Assembly of Poly(ferrocenyldimethylsilane-*b*-dimethylaminoethyl methacrylate): Toward Water-Soluble Cylinders with an Organometallic Core

Xiaosong Wang, Mitchell A. Winnik,* and Ian Manners*

Department of Chemistry, University of Toronto, 80 St. George Street, Toronto, Ontario, Canada M5S 3H6

Received January 30, 2004; Revised Manuscript Received December 10, 2004

ABSTRACT: Samples of the asymmetric block copolymer poly(ferrocenyldimethylsilane-*b*-dimethylaminoethyl methacrylate), PFS-*b*-PDMAEMA (block ratio ≈ 1:5), with a hydrophobic organometallic block and a hydrophilic organic block have been synthesized via a two-step anionic polymerization methodology. To study the self-assembly of these block copolymers in aqueous media, micelles were prepared by two different methods: selective precipitation involving the addition of water to PFS-*b*-PDMAEMA in dioxane and directly mixing water with PFS-*b*-PDMAEMA. In the selective precipitation experiments, the rate of water addition was found to be a crucial factor in determining the morphology of the resulting micellar structures. Rapid addition of water resulted in a monomodal distribution of solid spheres with an overall diameter of 20 nm, while slow addition created vesicle-like structures with a broad size distribution. Direct mixing of water with PFS-*b*-PDMAEMA led to even more complex micellization behavior. After PFS-*b*-PDMAEMA was initially dissolved in water, polydisperse spherical micelles with $R_h = \sim 65$ nm were formed. However, over time with constant stirring, a range of morphologies including spheres, rods, cylinders, and hollow structures were identified by electron microscopy, whereas, under quiescent conditions, the diameter of the spherical micelles gradually decreased to ca. 25 nm. Quaternization of the PDMAEMA blocks in PFS-*b*-PDMAEMA rendered a dramatic simplification to the micellization process. Only spheres were observed after the quaternized block copolymers were directly mixed with water. In contrast, alcohol solvents such as EtOH and ^{i}PrOH are able to induce PFS-*b*-PDMAEMA to self-assemble into cylindrical micelles by simply dissolving the block copolymers in the solvent. Aqueous colloidal solutions of cylindrical micelles could then be prepared via the dialysis of PFS-*b*-PDMAEMA in ethanol against water. The studies indicated that the solubility characteristics of the PDMAEMA corona chains in the micellization media exert a major influence on the micellization process and the resulting micellar morphologies.

Introduction

Self-assembly of diblock copolymers in selective solvents gives rise to micelle-like aggregates with the insoluble block as the core and the soluble block as the corona.[1,2] Although spheres are the most common morphology for block copolymer micelles, other types of supramolecular structures such as cylinders, lamellae, and vesicles[3,4] have been reported,[5,6] particularly for "crew-cut" systems where the soluble block is very short.[7] These nanoscale structures are of intense current interest and possess a range of potential applications in areas as diverse as nanolithography, impact modifiers for epoxy resins, and drug delivery.[8]

To date, the vast majority of studies have focused on all-organic systems. The incorporation of metals into block copolymer structures is of considerable interest for the generation of self-assembled supramolecular materials with novel physical and chemical properties.[9,10] The development of a living anionic ring-opening polymerization (ROP)[11] procedure for silicon-bridged [1]-ferrocenophanes (e.g., **1**) provides a convenient pathway to well-defined metal-containing polyferrocenylsilane (PFS) block copolymers such as PFS-*b*-PDMS (PDMS: polydimethylsilane) and PI-*b*-PFS (PI: polyisoprene). Such block copolymers are able to form micellar structures with a redox-active nanoscale organometallic core upon self-assembly in block-selective solvents. Generally, nonspherical morphologies, including cylinders,[12] tubes,[13] and ribbonlike platelets,[14] have been identified in studies of the solution self-assembly of either PFS-*b*-PDMS or PI-*b*-PFS block copolymers. The type of structure formed appears to depend on the block ratio and the nature of the soluble block. Crystallization of the PFS block has been proposed as the driving force for this unusual micellization behavior.[15] The combination of novel PFS properties,[9] such as redox activity and the ability to function as a magnetic ceramic precursor, and the intriguing micellar structures formed by its block copolymers offers interesting opportunities for a wide range of applications. For example, both PFS-*b*-PDMS and PI-*b*-PFS cylindrical micelles self-assembled in hexane have recently been shown to function as precursors to lithographically defined ceramic nanolines following a plasma etching procedure.[16] In addition, the corona of PI-*b*-PFS cylinders can be cross-linked by platinum-catalyzed hydrosilylation to afford permanent cylindrical nano-objects. These can be aligned using microfluidic channel methods and form magnetic ceramic replicas on pyrolysis.[17]

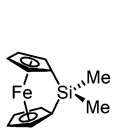

(**1**)

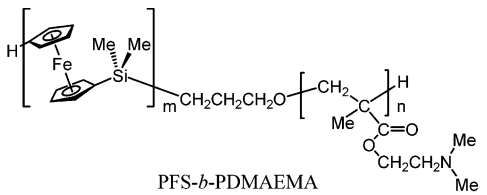

PFS-*b*-PDMAEMA

(**2**)

To facilitate further developments, water-soluble PFS micelles are desirable. In this regard, in a preliminary

10.1021/ma049793q CCC: $30.25
Published on Web 02/09/2005

Table 1. Characterization of PFS-*b*-PDMAEMA Block Copolymers

	PFS block[a]		PFS-*b*-PDMAEMA[a]		
samples	M_n	M_w/M_n	M_n	M_w/M_n	block ratio (M_n)[b]
PFS_9-*b*-$PDMAEMA_{50}$	2200	1.01	10 000	1.20	9:50 (10 000)
PFS_{11}-*b*-$PDMAEMA_{55}$	2800	1.02	11 000	1.30	11:55 (11 300)

[a] GPC with light scattering detector. [b] Calculated from ^{1}H NMR integration.

communication,[18] we reported the synthesis of amphiphilic PFS-*b*-PDMAEMA (PDMAEMA: polydimethylaminoethyl methacrylate) (**2**) block copolymers. PDMAEMA homopolymer is water soluble.[19] In this paper, we report the full details of the synthesis and characterization of these polymers and we describe their self-assembly in aqueous media.

Experimental Section

1. Materials and Characterization. Dimethylaminoethyl methacrylate was purchased from Aldrich and distilled over CaH_2 before polymerization. Decamethylferrocene was purchased from Aldrich and used as received. (*tert*-Butyldimethylsilyloxy)-1-propyl lithium (*t*-BDMSPrLi) was purchased from Polymer Source and used as received. The synthesis of highly pure [1]ferrocenophane (**1**) was described in our previous publication.[11b] PDMAEMA homopolymers (M_n = 5500, PDI = 1.30) were synthesized by ATRP according to the published literature.[10]

Molecular weights and molecular weight distributions were characterized by gel permeation chromatography (GPC) using a Waters Associates 2690 Separations Module equipped with Ultrastyragel columns with pore sizes of 10^3-10^5 Å, in-line degasser, and a differential refractometer. Polystyrene standards purchased from American Polymer Standards were used for calibration purposes. Alternatively, a Waters Associates liquid chromatograph equipped with a Waters 410 differential refractometer and a Viscotek T60A dual detector consisting of a 90° angle laser light scattering detector (λ_0 = 670 nm) and a four-capillary differential viscometer was used. The triple-detector system was used to provide absolute M_w values, and d*n*/d*c* was measured on-line. The instrument was calibrated with known d*n*/d*c* values of polystyrene standards.

Dynamic Light Scattering (DLS) experiments were carried out using an AVL-5000 instrument operating in the dynamic mode. The autocorrelation function was fitted by the CONTIN program. We performed all DLS experiments at 90° to obtain apparent hydrodynamic radius, except where otherwise indicated.

Transmission electron microscopy (TEM) measurements were carried out on a Hitachi model 600 electron microscope operating at 75 kV. The samples were prepared by aerosol spraying or by drying a drop of the micelle solution on a carbon-coated copper grid. For the negative-staining experiments, phosphotungstic acid was used as a staining agent.

2. Synthesis of PFS-*b*-PDMAEMA. *2.1. Synthesis of PFS−$CH_2CH_2CH_2$−OH (**3**).* In a glovebox at room temperature, 150 μL of 0.6 M *t*-BDMSPrLi (0.09 mmol) in cyclohexane was added quickly to a stirred solution of 250 mg of [1]silaferrocenophane (1.03 mmol) in THF (1.5 mL) at room temperature. After 30 min, the solution changed from a red to a deep amber color, and then a few drops of MeOH were added to terminate the polymerization. PFS with a *t*BDMS end group was isolated by precipitation of reaction mixture in methanol and dried at room temperature under vacuum overnight yielding 240 mg (96%). ^{1}H NMR ($CDCl_3$, 300 MHz): δ = 0.06 (s, 6H, Si−CH_3) 0.22 (s, 6H, C−Si−CH_3), 0.46 (s, 6H, −fcSi−CH_3), 0.71 (t, 2H, Si−CH_2), 0.97 (s, 9H, C−CH_3), 1.45 (m, 2H, C−CH_2), 3.40 (t, 2H, CH_2−O), 4.05 (m, 4H, Cp), 4.21 (m, 4H, Cp). GPC (in THF, light scattering detector): M_n = 2850, PDI = 1.1.

Siloxyl-terminated PFS (180 mg, 6.4 × 10^{-2} mmol) was dissolved in 5 mL of THF. To this solution, 5μL of 1.0 M $[Bu_4N]F$ THF solution was added. After being stirred for 24 h at room temperature, the reaction mixture was concentrated and then precipitated in methanol to recover **3**, which was dried at room temperature under vacuum overnight, yielding 170 mg (94%). ^{1}H NMR ($CDCl_3$, 300 MHz): δ = 0.22 (s, 6H, C−Si−CH_3), 0.46 (s, 6H, −fcSi−CH_3), 0.71 (t, 2H, Si−CH_2), 1.45 (m, 2H, C−CH_2), 3.40 (t, 2H, CH_2−O), 4.05 (m, 4H, Cp), 4.21 (m, 4H, Cp). GPC (in THF, light scattering detector): M_n = 2800, PDI = 1.02.

2.2. Synthesis of PFS-b-PDMAEMA. After 3 mg of KH (7.5 × 10^{-2} mmol) was weighed in a glovebox, the reaction flask with a stir bar and KH was placed on an Ar line, and then 170 mg of **3** (6.07 × 10^{-2} mmol) in 5 mL of THF was added via a cannula. The resulted dispersion was stirred for 30 min at 0 °C. Before the reaction was warmed to room temperature, 470 mg of DMAEMA monomer (2.99 mmol) was added quickly via a cannula, and polymerization was left for 2 h before being terminated by a small amount of methanol. The block copolymer was isolated by precipitation in hexane at room temperature followed by filtration and drying under vacuum at room-temperature overnight. An amber-colored solid was collected (600 mg, 93%). ^{1}H NMR ($CDCl_3$, 300 MHz): δ = 0.46 (s, 6H, Si−CH_3), 1.05 (m, 3H, C−CH_3), 1.90 (m, 2H, CH_2−C), 2.29 (s, 6H, N−CH_3), 2.57 (t, 2H, CH_2−N), 4.08 (t, 2H, CH_2−O), 4.01 (m, 4H, Cp), 4.21 (m, 4H, Cp). GPC results are compiled in Table 1.

3. Quaternization of PFS-*b*-PDMAEMA: Synthesis of PFS-*b*-qPDMAEMA. Quaternization of PDMAEMA blocks was performed through the reaction of PFS_9-*b*-$PDMAEMA_{50}$ (100 mg, 0.5 mmol amino groups) with excess CH_3I (142 mg, 1 mmol) in THF at 23 °C, resulting in quaternized analogues, PFS-*b*-qPDMAEMA, with quantitative yield (170 mg). Over 24 h of reaction time, PFS-*b*-qPDMAEMA precipitated out of THF due to its solubility decrease. The product were collected by filtration and washed with THF before drying under vacuum. The degree of quaternization was quantitative, as indicated by ^{1}H NMR in D_2O, which selectively solubilizes qPDMAEMA blocks. ^{1}H NMR (D_2O, 300 MHz): δ = 1.00 (m, 3H, C−CH_3), 1.90 (m, 2H, CH_2−C), 3.1 (s, 9H, N−CH_3), 3.7 (s, 2H, CH_2−N), 4.4 (s, 2H, CH_2−O).

4. Micelle Preparation. 4.1. Selective Precipitation Method. 4.1.1. Slow Addition of Water to a Polymer Solution. Method 1: To a solution of PFS-*b*-PDMAEMA in 1 mL of dioxane (1 mg/1 mL), water (10 mL) was added *dropwise* to selectively precipitate PFS blocks. Typically, one drop was added every 20 s. After all of the water was added, an aliquot (ca. 1.5 mL) of water/dioxane solution was taken and filtered for light scattering and TEM measurements. The remaining solution was dialyzed against water for 5 days to remove dioxane, and the external water was changed everyday. There was no detectable difference between the micelles before and after dialysis.

4.1.2. Rapid Mixing of Water with Polymer Solution. Method 2: This method is similar to the process described as Method 1, but water was added drop by drop *continuously* into the dioxane solution.

Method 3: This method is similar to Method 1, but instead of adding water to the dioxane solution, the dioxane solution was injected into water. This method always gave results identical to those of Method 2.

4.2. Direct Dissolution Method. Samples of PFS_9-*b*-$PDMAEMA_{50}$ (50 mg) were mixed directly with water (50 mL) at 23 °C with stirring by a magnetic bar. At certain time intervals, aliquots of solution for DLS and TEM analysis were taken and passed through a filter with 800 nm pores before characterization.

4.3. Formation of Aqueous Cylindrical Micelles. Samples of PFS_9-*b*-$PDMAEMA_{50}$ (10 mg) were mixed directly with ethanol (10 mL) and sonicated for 20 min, using a 60 W ultrasonic

Scheme 1

1. Synthesis and characterization of PFS-PDMAEMA

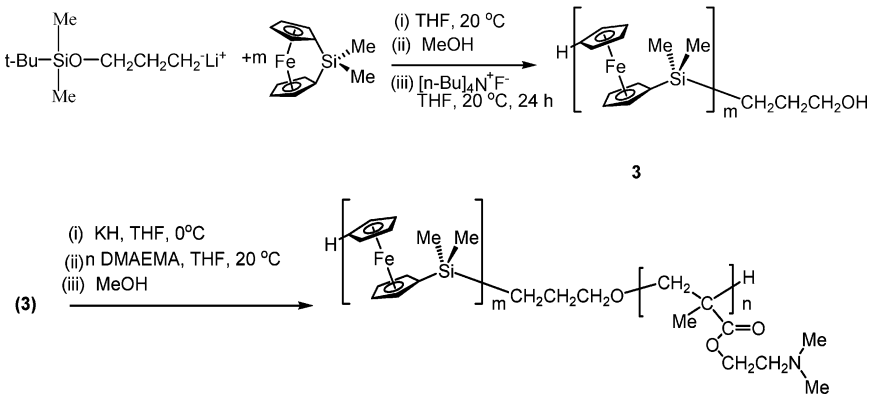

cleaning bath, to form a micelle solution. The resulting micelle solution was dialyzed against water that was changed every day for one week to transfer the micelles from ethanol to water. The hydrodynamic radii of the micelles before and after dialysis were identical, as characterized by DLS.

Results and Discussion

1. Synthesis and Characterization of PFS-*b*-PDMAEMA. The block copolymer poly(ferrocenyldimethylsilane-*b*-dimethylaminoethyl methacrylate), PFS-*b*-PDMAEMA was prepared by a two-step synthesis, as illustrated in Scheme 1. The steps consisted of the synthesis of hydroxy-terminated polyferrocenyldimethylsilane (PFS$-CH_2CH_2CH_2OH$) (**3**) followed by the polymerization of dimethylaminoethyl methacrylate (DMAEMA) initiated by PFS$-CH_2CH_2CH_2O^-K^+$, generated from the reaction of **3** with KH. Telechelic **3** was prepared by the (*tert*-butyldimethylsilyloxy)-1-propyl lithium (*t*-BDMSPrLi) initiated anionic ROP of **1** at room temperature. *t*-BDMSPrLi is well documented as a hydroxy-group-protected initiator for anionic polymerization,[21] where the *t*BDMS protecting group on the initiator is subsequently hydrolyzed to generate an $-OH$ functionality in the presence of $[Bu_4N]F$ at room temperature over a time period of 24 h. The molecular weight of **3** was measured by GPC with a light scattering detector before it was used as a macroinitiator for the polymerization of the PDMAEMA block. A slight excess of KH relative to **3** was used to ensure full conversion to PFS$-CH_2CH_2CH_2O^-K^+$ at 0 °C. As soon as PFS$-CH_2CH_2CH_2O^-K^+$ was generated, DMAEMA monomer was introduced to commence the room-temperature polymerization, which, after 2 h, was finally quenched with methanol. The reaction mixture was precipitated in hexane at room temperature to isolate the amber block copolymers. Two block copolymer samples were prepared using this approach (see Table 1). Molecular weights and molecular weight distribution were characterized by using GPC. Representative GPC traces are illustrated in Figure 1. Block ratios were calculated by comparing integrated ^1H NMR signals due to the PFS and PDMAEMA blocks. On the basis of the absolute degree of polymerization of the PFS blocks measured by both GPC and ^1H NMR, the segment length of PDMAEMA was estimated from the block ratio. All results are collected in Table 1.

2. Aqueous Self-assembly of PFS-*b*-PDMAEMA. *2.1. Solution Behavior of PFS-b-PDMAEMA in Dioxane.* Before micelles were prepared by selective precipitation, DLS measurements (90° detection) were carried out on a solution of PFS_9-*b*-$PDMAEMA_{50}$ in dioxane in order to verify whether the block copolymers were dissolved homogeneously. Surprisingly, a bimodal size distribution with $R_h = 4$ and 90 nm was detected (Figure 2a) on the basis of CONTIN fitting of the autocorrelation function. The small objects with R_h of 4 nm are of the size expected for PFS_9-*b*-$PDMAEMA_{50}$ unimer molecules, whereas the species with the larger R_h of 90 nm appear to be aggregates. The mass fraction of the aggregates, as calculated by the instrument software, was very small (<2 wt%), although they gave substantial scattering intensity due to their large size. Since PFS is redox active,[22] we suspected that the small amount of aggregates could result from the oxidation

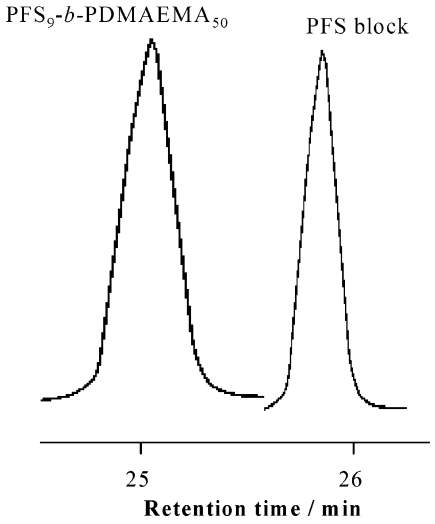

Figure 1. GPC traces for PFS_9-*b*-$PDMAEMA_{50}$ and its precursor.

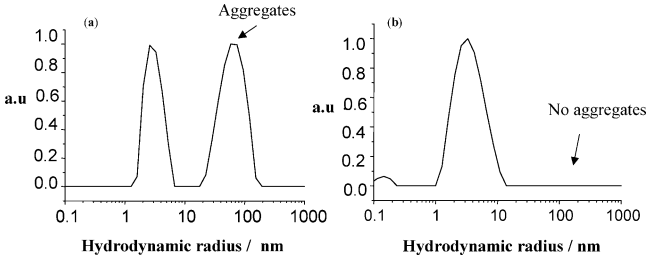

Figure 2. CONTIN plots of dynamic light scattering data for PFS_9-*b*-$PDMAEMA_{50}$ in dioxane (a) in the absence or (b) in the presence of decamethylferrocene. Solution concentration: 10 mg/mL.

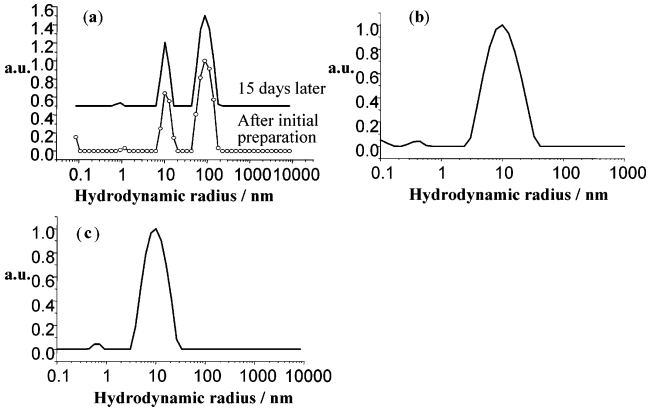

Figure 3. CONTIN plots of dynamic light scattering data for the micelles prepared by selective precipitation methods. (a) slow addition of water to a polymer solution in dioxane (Method 1), (b) rapid addition of water to a polymer solution in dioxane (Method 2) and (c) rapid addition of a polymer solution in dioxane to water (Method 3).

of main-chain ferrocene groups. The oxidation would create a polymer with ferrocenium sites, which would be expected to be less soluble and could prompt the formation of aggregates.

To test this idea, PFS_9-*b*-$PDMAEMA_{50}$ was dissolved in dioxane in the presence of decamethylferrocene, a reducing agent for ferrocenium sites. As shown in Figure 2b, the large R_h peak disappeared. Only a single peak was found, with R_h of ca. 4 nm corresponding to polymer unimers. The absence of aggregates in a PFS_9-*b*-$PDMAEMA_{50}$ dioxane solution containing a reductant supports the idea that oxidation of the PFS block in PFS_9-*b*-$PDMAEMA_{50}$ is the cause of the formation of small amount of aggregates in dioxane, a good solvent for both PDMAEMA and unoxidized PFS.

2.2. Aqueous Micellization Behavior of PFS-b-PDMAEMA. 2.2.1. Micelles Prepared by the Selective Precipitation Method. Since the mass of oxidation-induced PFS-*b*-PDMAEMA aggregates in dioxane was small, we prepared micelles by mixing water with PFS_9-*b*-$PDMAEMA_{50}$ dioxane solution without pretreatment to exclude the oxidized PFS units. Solutions of micelles at a concentration of ca. 1 mg/mL were prepared by either slowly or rapidly mixing water with dioxane solution. In the first method, micelles were prepared by adding water slowly (Method 1) in an attempt to make micelles under conditions that we hoped were close to equilibrium. Surprisingly, this slow process created a bimodal distribution of aggregates. As shown in Figure 3a, in addition to the aggregates with R_h of 10 nm, a small amount of large aggregates with $R_h \approx 100$ nm were formed. Both types of aggregates appear to be quite stable since there were no changes in the CONTIN plot when the solution was characterized 15 days later by DLS. The formation of bimodal aggregates could be prevented by mixing the water and polymer solutions rapidly, for example, by injecting water continuously into the dioxane solution (Method 2) or by injecting the dioxane solution into water (Method 3). As shown in Figure 3b and c, DLS characterization of the resulting micelle solutions indicated that only small aggregates with R_h of 10 nm were formed by either Method 2 or Method 3. When these structures were examined by TEM, spherical micelles were found. Representative TEM images are presented in Figure 4. As shown in Figure 4a for an unstained sample, solid spheres with diameters of around 4 nm were observed, corresponding

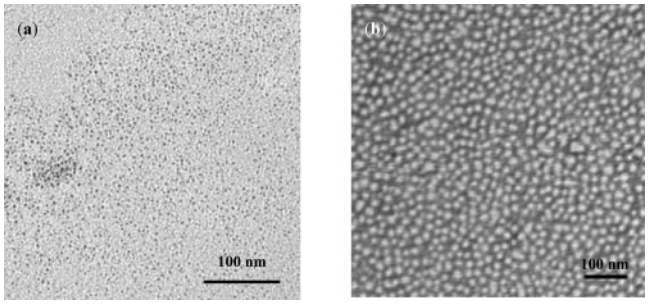

Figure 4. TEM images for the micelles prepared by selective precipitation of PFS blocks through the rapid addition of PFS_9-*b*-$PDMAEMA_{50}$ in dioxane to water (Method 3). (a) pristine sample and (b) negative stained sample using phosphotungstic acid.

to the electron-rich PFS cores of the micelles. An overall micelle diameter of ca. 20 nm was estimated by TEM from negative staining experiments (Figure 4b). These diameters are comparable to the values obtained from the DLS measurements.

Since we have shown that oxidation of the PFS block is able to induce aggregation of PFS-*b*-PDMAEMA in dioxane (see Figure 2), we initially considered the possibility that oxidation could be a reason for the formation of bimodal aggregates during the slow water addition process. To explore this possibility, we prepared micelles from the dioxane solution in the presence of a reductant, decamethylferrocene, to exclude oxidation-driven aggregation. The results were essentially identical to those experiments without reductant, namely bimodal aggregates were observed in the case of slow addition of water, while a monomodal size distribution was formed by the rapid addition of water.[23] The observation of similar micellization behavior despite the presence of a reductant suggests that the bimodal aggregation induced by the slow addition of water does not result from the oxidation of PFS.

A comparison of the various methods for making micelles showed that the rate of water addition was a factor strongly influencing the micellization behavior. Bimodal aggregates were detected only when water was added slowly (Method 1), while rapidly mixing water with the PFS-*b*-PDMAEMA solution in dioxane (Methods 2 and 3) led to a monomodal aggregate distribution. To elucidate the basis for this unusual phenomenon, DLS experiments were carried out to follow this slow water addition process. Figure 5 illustrates CONTIN fitting profiles of PFS_9-*b*-$PDMAEMA_{50}$ in dioxane solution with different amounts of added water. As we expected, when the polymer was initially dissolved in dioxane, small amounts of the aggregates were formed due to the existence of a small amount of oxidized PFS.

Upon the addition of one drop of water to 1 mL of the polymer solution (10 mg/mL), these aggregates dissociated, presumably due to the increased hydrophilicity of oxidized PFS (Figure 5a). After a second drop of water was added, a peak with R_h close to 100 nm appeared and its intensity increased steadily during the measurement. This result suggests that the peak is due to the aggregates that form slowly in the solution. After 15 h, when the intensity of the light scattering signal had leveled off, the CONTIN plot from the DLS measurement showed a substantial quantity of these initial aggregates (Figure 5b). At this point, the process of adding water was resumed. When a few more drops of water were added, the light scattering intensity in-

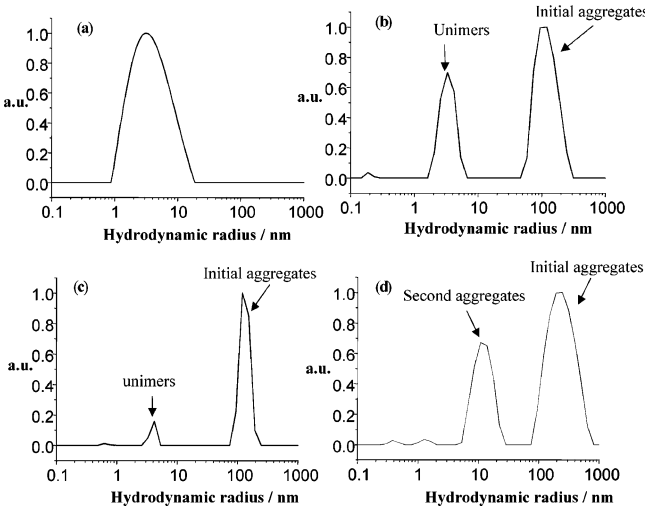

Figure 5. PFS_9-*b*-$PDMAEMA_{50}$ aggregation behavior examined by dynamic light scattering during selective precipitation involving slow addition of water dropwise (≈0.03 mL/drop) to a solution of the block copolymer in dioxane. ((a) one drop of water added, (b) 15 h later after second drop of water was added, (c) 7 drops of water added, and (d) 30 drops of water added).

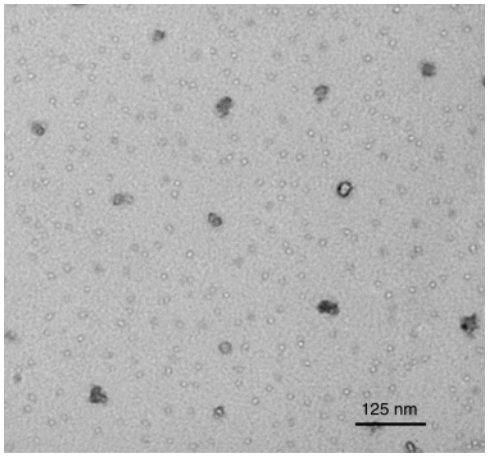

Figure 6. TEM image for the micelles prepared by selective precipitation involving slow addition of water to a solution of PFS_9-*b*-$PDMAEMA_{50}$ in dioxane. (Method 1).

creased further as more aggregates formed (Figure 5c). Only after 10 drops of water were added were we able to observe a peak in the CONTIN plot due to smaller aggregates with R_h ≈10 nm. Further addition of water led to a significant increase in the intensity of the peak due to the smaller aggregates with respect to that due to the initial aggregates (Figure 5d).

These DLS experiments as a function of water addition indicated that the water content in the solvent mixture dramatically influenced the micellization behavior. The large aggregates formed slowly, when the water content was low. As the water content was increased, no further formation of the large aggregates occurred and substantial amounts of the smaller aggregates started to form. If the water content of the system is increased rapidly (Method 2 or 3), the formation of initial large aggregates can be prevented.

TEM experiments on micelles prepared by Method 1, which have a bimodal size distribution as characterized by DLS (see Figure 3), were carried out to identify their structures. As shown in Figure 6, small spherical objects and larger aggregates were found to coexist. For the

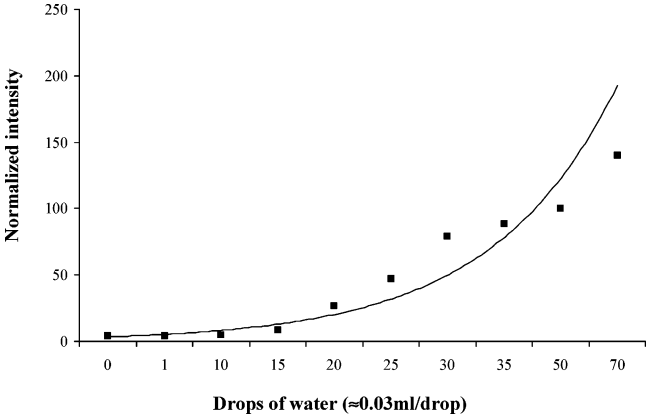

Figure 7. The effect of the addition of water on the light scattering intensity of PDMAEMA homopolymer in 1 mL of dioxane (5 mg/mL).

Figure 8. Possible structures for (a) apparently hollow micelles and (b) the spherical micelles observed by TEM.

small spheres representing the majority of structures, a dark circumference with diameter of 12 nm, corresponding to an electron-rich PFS region, and a bright center with a diameter of 4 nm were observed. Since PDMAEMA chains are not detected in these TEM experiments, the bright center could be either a PDMAEMA domain or a cavity. Outside the PFS dark region, a TEM-invisible PDMAEMA layer is expected to stabilize the micelles in water, which would lead to an overall diameter of around 20 nm, as indicated by DLS.

Since the micellization behavior and resulting micellar morphologies were controlled by the water addition rate, we suspected that the reason for the formation of different morphologies under different conditions might involve the solution behavior of the PDMAEMA block in the solvent mixture. Although PDMAEMA homopolymer is completely soluble in the individual solvents, water and dioxane, we were concerned that the polymer might have limited solubility in the mixture of solvents. For example, poly(*N*-isopropylacrylamide) is soluble in both water and methanol at room temperature but is insoluble in a 1:1 mixture.[24]

To gain further insight into these phenomena, we conducted DLS studies to follow the process of adding water to PDMAEMA homopolymer in dioxane. As shown in Figure 7, as water was added, the light scattering intensity increased, suggesting that aggregates of PDMAEMA were induced by the addition of small amounts of water to the dioxane solution. This experiment indicates that the presence of water can dramatically decrease the solubility of PDMAEMA in dioxane.

Therefore, the apparently hollow structures observed in Figure 6 may arise from the entrapment of PDMAEMA chains (see Figure 8a) due to the marginal solubility of PDMAEMA in the solvent mixture during

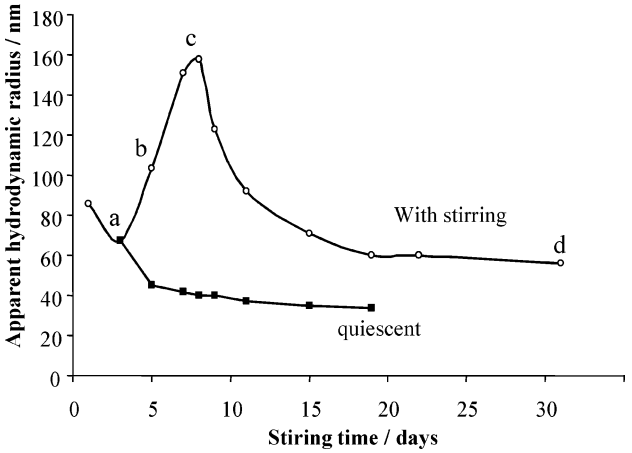

Figure 9. R_h of the micelles prepared by direct dissolution method through mixing PFS_9-*b*-$PDMAEMA_{50}$ with water under stirred or quiescent conditions as a function of micellization time.

the slow addition of water. This entrapment was apparently prevented in the case where water was added quickly because of rapid precipitation of the more strongly hydrophobic PFS chains, leading to more traditional spherical micelles with dense PFS cores (see Figure 8b). A more detailed investigation is necessary to understand this complex micellization process.

2.2.2. Direct Dissolution Method. We also explored the micellization of PFS_9-*b*-$PDMAEMA_{50}$ using an alternative sample preparation method. This involved directly mixing PFS_9-*b*-$PDMAEMA_{50}$ with water and stirring over a long period of time (ca. 30 days). At the end of the micellization process, samples of the block copolymers were recovered by removing water and were characterized by GPC and ^{1}H NMR. We obtained identical GPC traces and ^{1}H NMR spectra before and after preparing micelles, indicating that no detectable oxidation or degradation of the block copolymers occurred. Aliquots were taken over time and passed through 800 nm filters and then characterized by DLS. The resulting R_h values are plotted against micellization time in Figure 9. As shown in Figure 9, the stirred solution exhibited an unusual and striking increase in R_h over 10 days followed by a decrease to ca. 60 nm. We had expected that the shear forces associated with stirring would promote breakup of the aggregates. This experiment was repeated three times, and similar results were obtained each time.

For comparison, an aliquot of this micelle solution was removed after 3 days. This solution was kept under quiescent conditions and monitored by DLS. As shown in Figure 9, this solution behaved differently. The R_h value in this case gradually declined over time to a small value ($R_h \approx 30$ nm). The absence of an increase in R_h for the quiescent sample implies that stirring provides the shear force perturbing the aqueous micellization of PFS_9-*b*-$PDMAEMA_{50}$ and that this force is responsible for the evolution of R_h in the stirred solution.

TEM studies were carried out to explore the nature of the aggregates present in the stirred solutions. Samples were taken after 3, 6, 9, and 30 days, corresponding to points a, b, c, and d in Figure 9. These TEM images are presented in Figure 10a, b, c, and d, respectively.

As shown in Figure 10a, when PFS_9-*b*-$PDMAEMA_{50}$ was initially dissolved in water, polydisperse spherical particles were formed, with a PFS core diameter in the

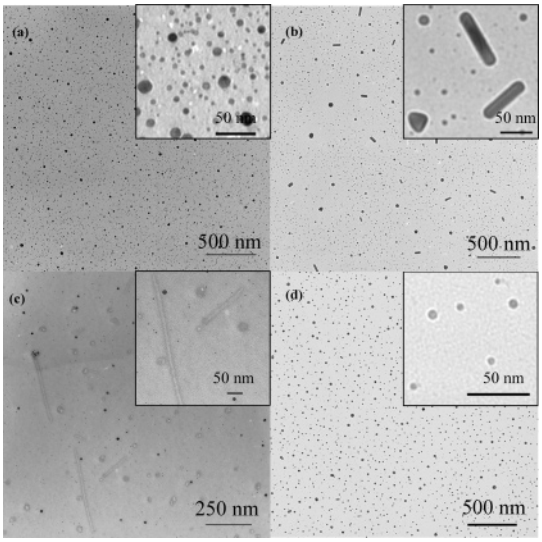

Figure 10. TEM analysis of the micelles prepared by direct dissolution method through stirring PFS_9-*b*-$PDMAEMA_{50}$ with water.

range of several tens of nanometers. Most of the structures look like solid spheres. For some micelles with a larger size, the center of the core seems brighter than its perimeter. Similar structures, but with relatively smaller size, were observed after micelle solution was stirred for a long period of time (see Figure 10d). A Pt/C shadowing TEM experiment of this sample following a long period of stirring indicated that the majority of the micelles in the solution had overall diameters of around 20 nm,[23] which is close to that for the micelles prepared by the selective precipitation method. A small amount of large aggregates was also observed in the TEM experiments, consistent with the large R_h value characterized by DLS.

Figure 10b shows the micelle structures in the sample taken at the time when DLS indicated an increase in R_h, corresponding to point b in Figure 8. As can be seen, rod structures were observed among the spheres. These rods had lengths of approximately 100 nm. Although rods were not the major structure formed, there were enough of them, and they were of sufficient size to change the light scattering signal from the solution.

When R_h reached its apex (point c in Figure 9), the TEM image (Figure 10c) showed that solid spheres and hollow structures coexist. The hollow structures consisted of spherical (vesicle-like) structures and rigid tubes. Compared with the solid rods formed at early stages in the experiment, the hollow cylinders were longer, with lengths up to 300 nm, which may account for the large R_h detected by DLS.

2.3. Aqueous Micellization of PFS_{11}-b-$PDMAEMA_{55}$. The unexpected micellization behavior of PFS_9-*b*-$PDMAEMA_{50}$ block copolymer was also found for other polymer samples with a similar block ratio. For example, the micellization behavior of PFS_{11}-*b*-$PDMAEMA_{55}$ (PDI = 1.30) was similar to that for PFS_9-*b*-$PDMAEMA_{50}$ (PDI = 1.20). Either solid or hollow spherical structures were observed by TEM from samples obtained by the selective precipitation method, depending on the rate of water addition, while a variety of morphologies including spheres, cylinders, and hollow structures were observed in the process of directly stirring the solid block copolymers with water. However, unlike the PFS_9-*b*-$PDMAEMA_{50}$ sample, even after a

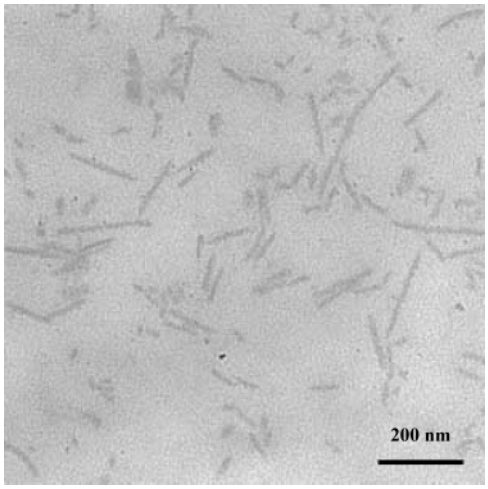

Figure 11. TEM for micelles prepared by direct dissolution method through stirring PFS_{11}-*b*-$PDMAEMA_{55}$ with water.

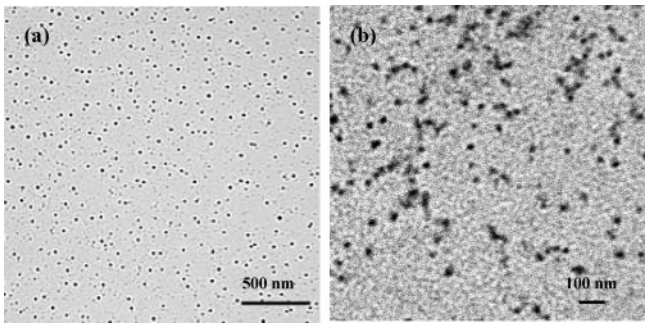

Figure 12. TEM for micelles prepared by direct dissolution method through stirring PFS_9-*b*-$qPDMAEMA_{50}$ with water. (a) Low magnification (b) high magnification.

long time stirring, TEM images of samples taken from the solution still showed complicated multiple morphologies, including cylinders and spheres, as shown in Figure 11.

2.4. Micellization of Quaternized PFS_9-b-$qPDMAEMA_{50}$. Upon quaternization of the PDMAEMA block (qPDMAEMA), the solubility of this organic block in water should be enhanced. Quaternization was achieved by reaction with methyl iodide in THF and proceeded to completion based on ^{1}H NMR analysis. As a result, the block copolymers were readily dispersed in water by directly mixing the dry polymer with water, and the micellization behavior was simplified. Figure 12 shows TEM images of the micelles. As can been seen from an image recorded at a low magnification (Figure 12a), the overall micellar structures look like spheres with an apparently relatively narrow size distribution. An image taken at a relatively high magnification gives us a chance to view the structures in more detail. The diameters of the dark structures in Figure 12b range from 12 to 58 nm. These dark objects correspond to the PFS component of the self-assembled structures present on the TEM grid. The large particles are likely due to the aggregates of micelles, which formed during the preparation of the TEM sample from a drop of the micelle solution. However, we cannot rule out the possibility that the aggregation of micelles occurred in solution state.

The micelle solution was examined by angular-dependent DLS. At each scattering angle, the CONTIN plots showed the presence of a single species with a narrow distribution of relaxation rates (PDI = 0.12 from the cumulant analysis). The plot of the first cumulant vs q^2 was linear and passed through the origin.[23] From this plot, we calculated an apparent hydrodynamic radius of 29 nm. This value seems large, considering the length of the qPDMAEMA chains and the small size of the core for the majority of the micelles. The anomaly in the observation can probably be accounted for by the existence of aggregates of micelles in the solution perhaps similar to those seen in the TEM images of Figure 12b. It is also possible that a small but significant amount of micellar aggregates might dominate the light scattering signal, leading to information only about the large particles present in solution.

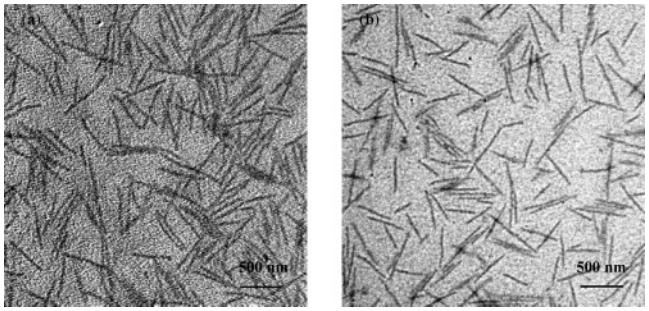

Figure 13. TEM for the micelles prepared by (a) mixing PFS_9-*b*-$PDMAEMA_{50}$ with ethanol and (b) replacing ethanol with water by dialysis

2.5. Self-Assembly in Ethanol: Formation of Aqueous Solutions of Cylindrical Micelles of PFS-b-PDMAEMA. The complex micellization behavior of PFS-*b*-PDMAEMA that we observed in samples prepared by stirring with water might be due to a marginal water solubility of PDMAEMA and a hydrophobicity of PFS chains. To test this hypothesis, we carried out micellization experiments with PFS-*b*-PDMAEMA using alcohol solvents. Here we obtained micelles in the form of uniform cylinders. We obtained similar structures for methanol, ethanol, and 2-propanol as solvents. In Figure 13a, we show TEM images of cylinders of PFS_9-*b*-$PDMAEMA_{50}$ formed in ethanol. A more detailed description of micellization experiments carried out in alcohol solvents will be published separately. Dialysis of the micelles in ethanol against water successfully allowed the transfer of the cylinders into water. A TEM image of the structures present in water after preparation in ethanol is shown in Figure 13b. We initially suspected, on the basis of our previous studies, that the formation of cylinders might be due to the crystallization of PFS.[15] However, preliminary studies involving a WAXS experiment carried out on a solid film sample of the cylindrical micelles, prepared by evaporating ethanol, did not reveal any clear PFS diffraction peak.

Conclusions

Aqueous micellization of PFS-*b*-PDMAEMA was studied by a combination of dynamic light scattering and transmission electron microscopy. We found unusual structures, and for some sample preparation methods, complex micellization behavior.

1. PFS-*b*-PDMAEMA aggregates were detected in dioxane, a common solvent for both blocks, due to the presence of a small amount of oxidized PFS.

2. The water addition rate was found to influence the micelle morphology, when micelles were prepared by the selective-precipitation method. Normal starlike spherical micelles were formed when solutions of the polymer

in dioxane were mixed quickly with water, whereas vesicle-like structures were generated by the slow addition of water to the polymer solution. Poor solubility of PDMAEMA chains in dioxane in the presence of small amounts of water was identified as the major reason for this unexpected behavior.

3. A variety of morphologies including rods, cylinders, and hollow structures were observed during experiments in which solutions were prepared by directly mixing the polymer with water with stirring. Stirring appears to promote the slow aggregation process (over days) followed by breakup of the aggregates.

4. Quaternization of the PDMAEMA block simplified the micellization of the block copolymer in water. Only spherical micelles were observed.

5. When PFS-*b*-PDMAEMA was dissolved in an alcohol solvent, such as ethanol, cylindrical micelles with an apparently amorphous PFS core formed.[25] These structures remained unchanged when they were transferred via dialysis to water.

Further detailed studies of the self-assembly of PFS-*b*-PDMAEMA in alcohol solvents are underway in an attempt to understand the factors that determine the morphologies observed. These results will be reported in a future publication.

Acknowledgment. M.A.W. and I.M. thank the Emerging Materials Knowledge program of Materials and Manufacturing Ontario for funding.

Supporting Information Available: Hydrodynamic radii, TEM images, angular-dependent DLS studies, and d*n*/d*c* calculation procedure. This material is available free of charge via the Internet at http://pubs.acs.org.

References and Notes

(1) Hamley, I. W. *The Physics of Block Copolymers*; Oxford University Press, Inc.: New York, 1998.
(2) (a) Halperin, A.; Tirrell, M.; Lodge T. P. *Adv. Polym. Sci.* **1992**, *100*, 31. (b) Simon, P. F. W.; Ulrich, R.; Spiess, H. W.; Wiesner, U. *Chem. Mater.* **2001**, *13*, 3464. (c) Choucair, A.; Eisenberg, A. *Eur. Phys. J. E* **2003**, *10*, 37.
(3) (a) Jenekhe, S. A.; Chen, X. L. *Science* **1998**, *279*, 1903. (b) Discher, D. E., Eisenberg, A. *Science* **2002**, *297*, 967.
(4) (a) Tao, J.; Stewart, S.; Liu, G.; Yang, M. *Macromolecules* **1997**, *30*, 2738. (b) Stewart, S.; Liu, G. *Angew. Chem. Int. Ed.* **2000**, *39*, 340.
(5) (a) Jain, S.; Bates, F. S. *Science* **2003**, *300*, 460. (b) Won, Y.; Davis, H. T.; Bates, F. S. *Science* **1999**, *283*, 960. (c) Discher, B. M.; Won, Y.; Ege, D. S.; Lee, J. C−M.; Bates, F. S.; Discher, D. E.; Hammer, D. A. *Science* **1999**, *284*, 1143. (d) Pochan, D. J.; Chen, Z. Y.; Cui, H. G.; Hales, K.; Qi, K.; Wooley, K. L. *Science* **2004**, *306*, 94. (e) Li, Z.; Kesselman, E.; Talmon, Y.; Hillmyer, M. A.; Lodge, T. P. *Science* **2004**, *306*, 98.
(6) (a) Antonietti, M.; Förster, S. *Adv. Mater.* **2003**, *15*, 1323. (b) Spatz, J. P.; Moessmer, S.; Möller, M. *Angew. Chem., Int. Ed. Engl.* **1996**, *35*, 1510.
(7) (a) Zhang, L.; Eisenberg, A. *Science* **1995**, *268*, 1728. (b) Zhang, L.; Eisenberg, A. *J. Am. Chem. Soc*. **1996**, *118*, 3168.
(8) For an example as drug delivery, see: (a) Savic, R.; Luo, L.; Eisenberg, A.; Maysinger, D. *Science* **2003**, *300*, 615. For an example as impact modifiers, see: (b) Dean, J. M.; Verghese, N. E.; Pham, H. Q.; Bates, F. S. *Macromolecules* **2003**, *36*, 9267−9270. (c) Goren, M.; Lennox, R. B. *Nano Lett.* **2001**, *1*, 735. For selected reviews, see: (d) Förster, S.; Antonietti, M. *Adv. Mater*. **1998**, *10*, 195. (e) Hamley, I. W. *Angew. Chem. Int. Ed.* **2003**, *42*, 1692. (f) Lazzari, M.; López-Quintela, M. A. *Adv. Mater.* **2003**, *15*, 1583.
(9) Manners. I. *Science* **2001**, *294*, 1664.
(10) (a) Gohy, J.-F.; Lohmeijer, B. G. G.; Varshney, S. K.; Schubert, U. S. *Macromolecules* **2002**, *35*, 7427. (b) Hou, S.; Man K. Y. K.; Chan, W. K. *Langmuir* **2003**, *19*, 2485.
(11) (a) Rulkens, R.; Ni, Y.; Manners, I. *J. Am. Chem. Soc.* **1994**, *116*, 12121. (b) Ni, Y.; Rulkens, R.; Manners, I. *J. Am. Chem. Soc.* **1996**, *118*, 4102.
(12) Massey, J. A.; Power, K. N.; Manners, I.; Winnik, M. A. *J. Am. Chem. Soc.* **1998**, *120*, 9533.
(13) Raez, J.; Manners, I.; Winnik, M. A. *J. Am. Chem. Soc.* **2002**, *124*, 10381.
(14) Cao, L.; Manners, I; Winnik, M. A. *Macromolecules* **2002**, *35*, 8258.
(15) Massey, J. A.; Temple, K.; Cao, L.; Rharbi, Y.; Raez, J.; Winnik, M. A.; Manners, I. *J. Am. Chem. Soc.* **2000**, *122*, 11577.
(16) (a) Massey, J. A.; Winnik, M. A.; Manners, I.; Chan, V. Z−H.; Ostermann, J. M.; Enchelmaier, R.; Spatz, J. P.; Möller, M. *J. Am. Chem. Soc.* **2001**, *123*, 3147. (b) Cao L.; Massey, J. A.; Winnik, M. A.; Manners, I.; Riethmuller, S.; Banhart F.; Spatz, J. P.; Möller, M. *Adv. Funct. Mater*. **2003**, *13*, 271.
(17) Wang, X. S.; Arsenault, A.; Ozin, G. A.; Winnik, M. A.; Manners, I. *J. Am. Chem. Soc.* **2003**, *125*, 12686.
(18) Wang, X. S.; Winnik, M. A.; Manners, I. *Macromol. Rapid Commun*. **2002**, *23*, 210.
(19) Gohy, J. F.; Antoun, S.; Jerome, R. *Macromolecules* **2001**, *34*, 7435.
(20) Wang, X. S.; Armes, S. P. *Macromolecules* **2000**, *33*, 6640.
(21) (a) Quirk, R. P.; Jang, S. H.; Yang, H. M.; Lee, Y. *Macromol. Symp.* **1998**, *132*, 281. (b) Zhang, P.; Moore, J. S. *J. Polym. Sci., Part A* **2000**, *38*, 207.
(22) (a) Foucher, D. A.; Nelson, J. M.; Honeyman, C.; Tang, B. Z.; Manners, I. *Angew. Chem. Int. Ed.* **1993**, *32*, 1709. (b) Cyr, P. W.; Tzolov, M.; Manners, I.; Sargent, E. H. *Macromol. Chem. Phys*. **2003**, *204*, 915. (c) Mang, Y. Q.; Cervantes-Lee, F.; Pannell, K. H. *Organometallics* **2002**, *21*, 5859.
(23) See Supporting Information.
(24) Winnik, F. Ringsdorf, M.; H.; Venzmer, J. *Macromolecules* **1990**, *23*, 2415.
(25) For related metallized nanocylinders, see: (a) Braun, E.; Eichen, Y,; Sivan, U.; Ben-Yoseph G.; *Nature* **1998**, *391*, 775. (b) Fullam, S.; Cottell, D.; Rensmo, H.; Fitzmaurice, D. *Adv. Mater.* **2000**, *19*, 1430. (c) Djalali, R.; Li, S. Y.; Schmidt, M. *Macromolecules* **2002**, *35*, 4282.

MA049793Q